DRAFT: The Spitzer Extragalactic Representive Volume Survey (SERVS): survey definition and goals

M. Lacy[1], D. Farrah[2], J.-C. Mauduit[3], J.A. Surace[3], G. Zeimann[4], M. Huynh[3], M. Jarvis[5], C. Maraston[6], S. Oliver[2], S.A. Stanford[4,7], E.A. Gonzáles-Solares[8], L. Marchetti[9], J. Pforr[6], M. Vaccari[9], J. Afonso[10,35], D.M. Alexander[11], R.H. Becker[4,7], P.N. Best[12], L. Bizzocchi[10,35], D. Bonfield[5], S. Bursick[13], N. Castro[14], A. Cava[14], S. Chapman[8], N. Christopher[15], D.L. Clements[16], J.S. Dunlop[12], E. Dyke[5], A. Edge[20], J.T. Falder[5], H.C. Ferguson[17], S. Foucaud[18], A. Franceschini[9], R.R. Gal[19], J.E. Geach[20], J.K. Grant[21], M. Grossi[10,35], E. Hatziminaoglou[22], B. Henriques[2], S. Hickey[5], R.J. Ivison[12], M. Kim[1], O. LeFevre[23], M. Lehnert[24], C.J. Lonsdale[1], L.M. Lubin[4], R.J. McLure[12], H. Messias[10,35], A. Martínez-Sansigre[6,15] A.M.J. Mortier[12], D.M. Nielsen[25], R.P. Norris[26], M. Ouchi[27], G. Parish[5], I. Perez-Fournon[14], A.O. Petric[3], M. Pierre[28], S. Rawlings[15], A. Readhead[29], A. Rettura[13], G.T. Richards[30], S.E. Ridgway[25], A.K. Romer[2], I.G. Rosebloom[2], H.J.A. Rottgering[31], M. Rowan-Robinson[16], A. Sajina[32], N. Seymour[33], C.J. Simpson[34], I. Smail[20], G.K. Squires[3], J.A. Stevens[5], R. Taylor[21], P.A. Thomas[2], M. Trichas[16], T. Urrutia[3], E. van Kampen[22], A. Verma[15], G. Wilson[13], C.K. Xu [3]

[1]National Radio Astronomy Observatory, 520 Edgemont Road, Charlottesville, VA 22903, USA

[2]Department of Physics and Astronomy, University of Sussex, Falmer, Brighton, BN1 9QH, UK

[3]Infrared Processing and Analysis Center/Spitzer Science Center, California Institute of Technology, Mail Code 220-6, Pasadena, CA 91125, USA

[4]Department of Physics, University of California, One Shields Avenue, Davis, CA95616, USA

[7]Center for Astrophysics Research, University of Hertfordshire, Hatfield, AL10 9AB, UK

[6]Institute of Cosmology and Gravitation, University of Portsmouth, Dennis Sciama Building, Burnaby Road, Portsmouth, PO1 3FX, UK

[7]IGPP, Lawrence Livermore National Laboratory, 7000 East Avenue, Livermore, CA94550, USA

[8]Institute of Astronomy, University of Cambridge, Madingley Road, Cambridge, CB3 0HA, UK

[9]Department of Astronomy, vic. Osservatorio 3, 35122, Padova, Italy

[10]Observatório Astronómico de Lisboa, Faculdade de Cência, Universidade de Lisboa, Tapada de Ajuda, 1349-018, Lisbon, Portugal

[11]Department of Physics, University of Durham, South Road, Durham, DH1 3LE, UK

[12]Institute for Astronomy, University of Edinburgh, Royal Observatory, Blackford Hill, Edinburgh, EH9 3HJ, UK

[13]Department of Physics and Astronomy, University of California-Riverside, 900 University Avenue, Riverside, CA92521, USA

[14]Institutio de Astrofísica de Canarias, C/Vía Láctea s/n, 38200, La Laguna, Tenerife, Spain

[15]Oxford Astrophysics, Denys Wilkinson Building, Keble Road, Oxford, OX1 3RH, UK

[16]Astrophysics Group, Blackett Laboratory, Imperial College, Prince Consort Road, London, SW7 2BW, UK

[17]Space Telescope Science Institute, 3700 San Martin Drive, Baltimore, MD 21218, USA

[18]School of Physics and Astronomy, University of Nottingham, University Park, Nottingham NG7 2RD, UK

[19]Institute for Astronomy, University of Hawaii, 2680 Woodlawn Drive, Honolulu, HI 96822, USA

[20]Institute for Computational Cosmology, Department of Physics, Durham University, South Road, Durham, DH1 3LE, UK

[21]Institute for Space Imaging Science, University of Calgary, AB T2N 1N4, Canada

[22]European Southern Observatory, Karl-Schwartzschild-Str. 2, 85748, Garching, Germany

[23]Laboratoire d'Astrophysique de Marseille, Traverse du Siphon, B.P.8, 13376 Marseille Cedex 12, France

[24]Laboratoire d'Etudes des Galaxies, Etoiles, Physique et Instrumentation GEPI, UMR8111, Observatoire

ABSTRACT

We present details of the *Spitzer Extragalactic Representative Volume Survey* (SERVS), an 18deg^2 medium-deep survey at 3.6 and 4.5μm with the post-cryogenic *Spitzer Space Telescope* to $\approx 2\mu$Jy ($AB = 23.1$) depth. SERVS is designed to enable the study of galaxy evolution as a function of environment from $z \sim 5$ to the present day, and is the first extragalactic survey both large enough and deep enough to put rare objects such as luminous quasars and galaxy clusters at $z \gtrsim 1$ into their cosmological context. SERVS is designed to overlap with several key surveys at optical, near- through far-infrared, submillimeter and radio wavelengths to provide a coherent picture of the formation of massive galaxies. In this paper, we discuss the SERVS data, ancillary data from other surveys in the SERVS fields (both already complete and in progress), and outline the main science topics that SERVS will address.

Subject headings: Astrophysical data

---

de Paris, Meudon, 92195, France

[25]Cerro Tololo Interamerican Observatory, Colina El Pino s/n, Casilla 603, La Serena, Chile

[26]CSIRO Australia Telescope National Facility, PO Box 76, Epping, NSW, 1710, Australia

[27]Observatories of the Carnegie Institute of Washington, 813 Santa Barbara Street, Pasadena, CA 91101, USA

[28]CEA, Saclay, F-91191 Gif-sur-Yvette, France

[29]California Institute of Technology, 2500 East California Boulevard, Pasadena, CA91125, USA

[30]Department of Physics, Drexel University, 3141 Chesnut Street, Philadelphia, PA 19014, USA

[31]Leiden Observatory, Leiden University, Oort Gebouw, PO Box 9513, 2300 RA Leiden, The Netherlands

[32]Department of Physics and Astronomy, Haverford College, Haverford, PA, 19041, USA

[33]Mullard Space Science Laboratory, UCL, Holmbury St Mary, Dorking, Surrey, RH5 6NT

[34]Astrophysics Research Institute, Liverpool John Moores University, Twelve Quays House, Egerton Wharf, Birkenhead CH41 1LD

[35]Centro de Astronomia da Universidade de Lisboa, Lisbon, Portugal

1. Introduction

Progress in extragalactic astronomy has been greatly enhanced by deep surveys such as the Great Observatories Origins Deep Survey (GOODS, Dickinson et al. 2003) and *Spitzer*-COSMOS (S-COSMOS, Sanders et al. 2007) that have allowed us to study the evolution of galaxies from the earliest cosmic epochs. A limitation of such surveys is, however, the relatively small volumes probed, even at high redshifts. For example, Ilbert et al. (2006) find field-to-field variations in redshift distributions noticable in the CFHTLS in fields of 0.7-0.9deg^2.

Until lately, howvever, the combination of depth and area required to map a large volume ($\sim$ 1Gpc^3) of the high redshift Universe at the near-infrared wavelengths, where the redshifted emission from stars in distant galaxies peaks, has been prohibitively expensive in telescope time. Two recent developments have, however, made this regime accessible. On the ground, the availabilty of wide-field near-infrared cameras has greatly improved the effectiveness of ground-based near-infrared surveys at 1-2.5μm wavelength range. In space, the exhaustion of the cryogenic coolant of the *Spitzer Space Telescope* opened up an opportunity to undertake surveys with the shortest wavelength two channels ([3.6] and [4.5]) of the Infrared Array Camera (IRAC, Fazio et al. 2004) in the post-cryogenic, or "warm" mission that were much larger than feasible during the cryogenic mission. These two developments led us to propose the *Spitzer Extragalactic Representative Volume Survey* (SERVS) as a *Spitzer* "Exploration Science" program.

SERVS is an 18deg^2 survey to $\approx 2\mu$Jy in the *Spitzer* [3.6] and [4.5] bands, which has been allocated 1400hr of telescope time over two years . (At the time of writing, approximately 60% of the data has been taken). SERVS samples $\sim$ 0.8Gpc^3 between redshift one and five. The five SERVS fields are centered on or close to those of corresponding fields surveyed by the shallower *Spitzer* Wide-area Infrared Extragalactic Survey (SWIRE; Lonsdale et al. 2003) fields, and picked to overlap with several other major surveys covering wavelengths from the X-ray to the radio. Of particular importance is near-infrared data, as these allow accurate photometric redshifts to be obtained. SERVS overlaps exactly with the 12deg^2 of the VISTA VIDEO survey in the South, and is covered by the UKIDSS DXS survey in the North. SERVS also has good overlap with the *Herschel* Multi-tiered Extragalactic Survey (HerMES) in the far-infrared, which covers the SWIRE and other *Spitzer* survey fields, with deeper subfields within many of the SERVS fields.

This paper is designed for use as a resource for papers making use of early data from SERVS, as well as warm *Spitzer* data in general. In this paper, we describe the survey fields, listing the existing or planned multiwavelength datasets that SERVS overlaps with. We outline the observational strategy and describe the first of the SERVS observations, and

their analysis. We also discuss the scientific aims of the survey.

2. Survey description

2.1. SERVS in context

SERVS is designed to open up a medium-depth, medium area part of parameter space in the mid-infrared (Fig. 1). The survey is designed to be large enough to contain significant numbers of rare objects, such as luminous quasars, Ultraluminous Infrared Galaxies (ULIRGS), radio galaxies and galaxy clusters, while still being deep enough to find L^* galaxies out to $z \approx 5$. Each of the five SERVS fields is between 2 and 4.5 deg^2 in area, with linear dimensions 1.4-3 deg.. For comparison, the largest structures seen in the Millenium simulation at $z \sim 1$ are $\sim$ 100Mpc (Springel et al. 2005), which subtends 3 deg. at that redshift, so each SERVS field should sample a wide range of environments. By combining the five different fields of SERVS, we will be able to effectively average over large-scale structure, and present a true picture of the average properties of galaxies in the high redshift Universe.

2.2. Fields

SERVS consists of five fields near the centers of corresponding SWIRE fields, ELAIS-S1 (hereafter ES1), XMM-LSS, CDFS, Lockman and ELAIS-N1 (hereafter EN1) (details in Tables 1 and 2). The SWIRE fields were chosen to be in regions with low infrared backgrounds, making them ideal for follow-up at far-infrared wavelengths. The SERVS fields were chosen to have good overlap with current and proposed surveys in other wavebands within the SWIRE fields, to cover both northern and southern hemispheres, and to have a range in Right Ascension allowing both flexible followup with ground-based telescopes and good scheduling opportunities for *Spitzer*. The fields are shown in Figures 2-4, together with the coverage of significant overlapping surveys.

2.3. Design of observations

The design of the SERVS observations reflected several trade-offs to ensure both efficient use of the telescope, accurate filling of the fixed field geometries, and reasonably flexible scheduling.

We elected to observe each field in two distinct epochs. The difference in time between

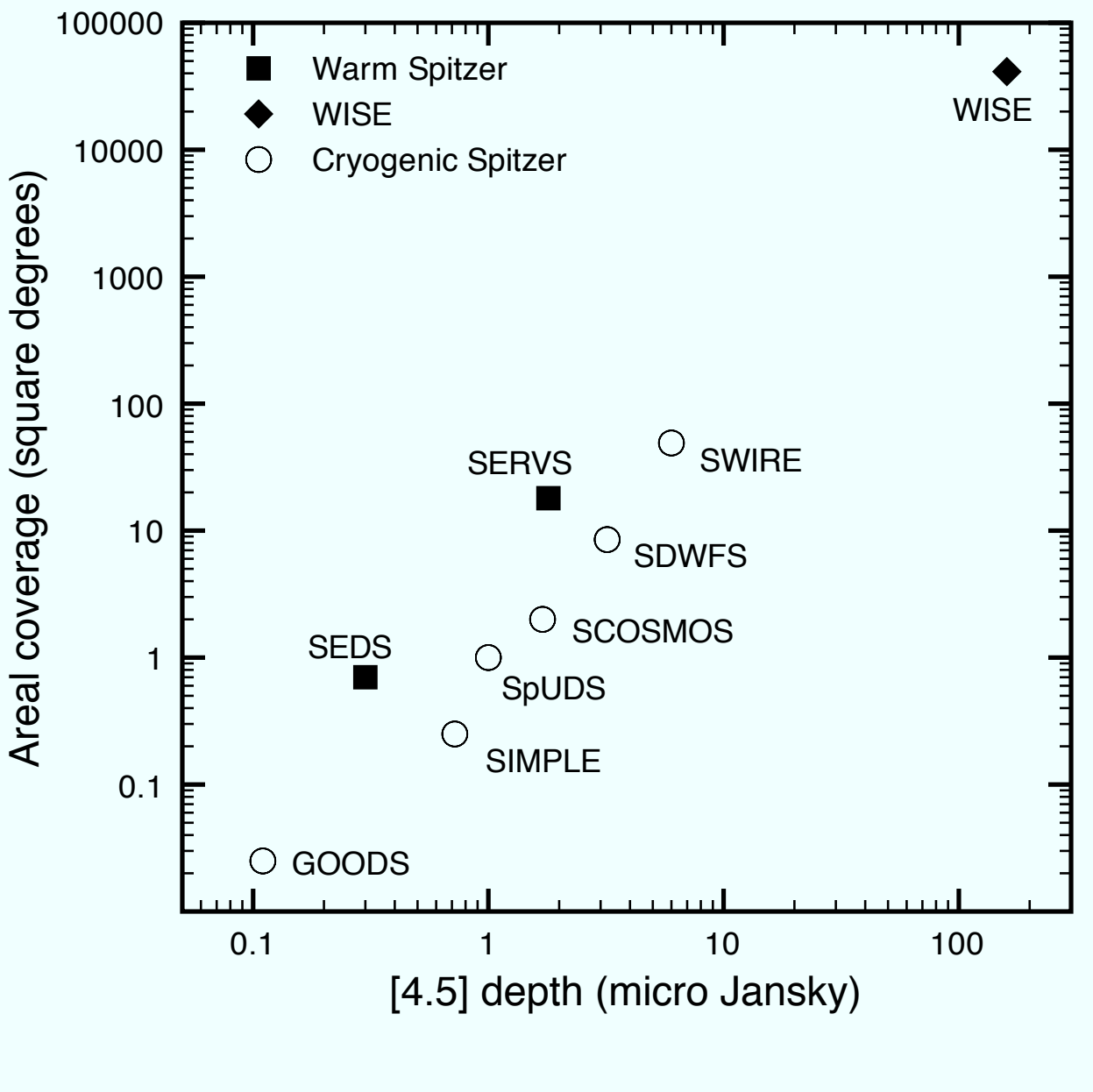

Fig. 1.— Area versus depth for SERVS compared to other surveys at wavelengths of $\approx 4.5\mu$m. For consistency, the depth shown is the 5σ limiting flux for point sources, excluding confusion noise ($\sigma_{\rm pp}$ as described in Section 5), calculated from the *Spitzer* performance estimation tool (http://ssc.spitzer.caltech.edu/warmmission/propkit/pet/senspet/index.html) in each case. The surveys are: GOODS, the *Spitzer* IRAC/MUSYC Public Legacy in E-CDFS (SIMPLE) survey (*Spitzer* program identifier [PID] 20708), the *Spitzer* Ultra Deep Survey (SpUDS, PID 40021, P.I. J.S. Dunlop), S-COSMOS, the *Spitzer* Deep Wide-Field Survey (SDWFS, Ashby et al. 2009), SWIRE and the *Spitzer* Extragalactic Deep Survey (SEDS, PIDs 60022, 61040, 61041, 61042, 61043 P.I. G. Fazio). The point for the Wide-Field Infrared Explorer (WISE) is the band 2 depth from Mainzer et al. (2005).

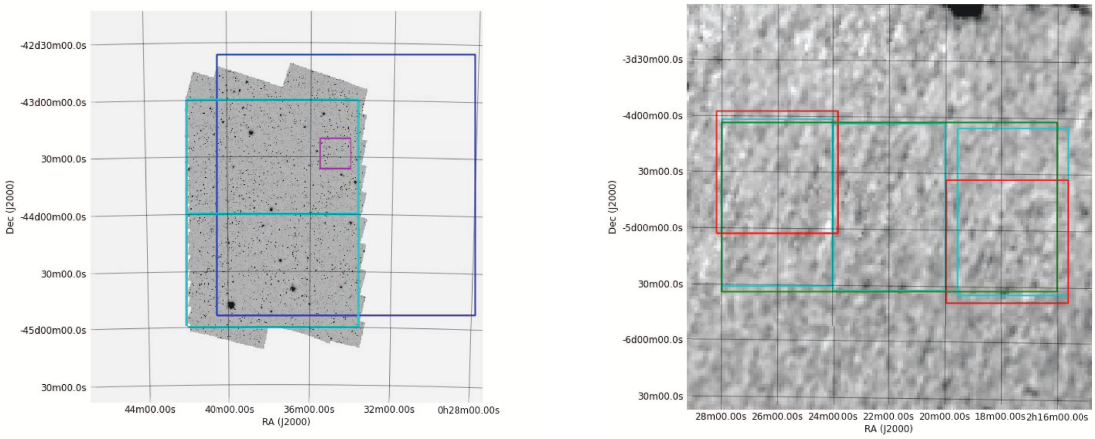

Fig. 2.— *Left* the [3.6] SERVS image of the ELAIS-S1 field. Superposed are the two VIDEO pointings (in cyan), the ATLAS radio survey (in blue) and the deep XMM field of Feruglio et al. (2008) (magenta). *Right* the IRAS 25μm image of the XMM-LSS field (the SERVS data for XMM-LSS is yet to be taken). The SERVS field is in green, the VIDEO pointings in cyan and the two HerMES level 5 pointings in red, the western pointing corresponds approximately to the VVDS, the eastern to the UDS/SpuDS field.

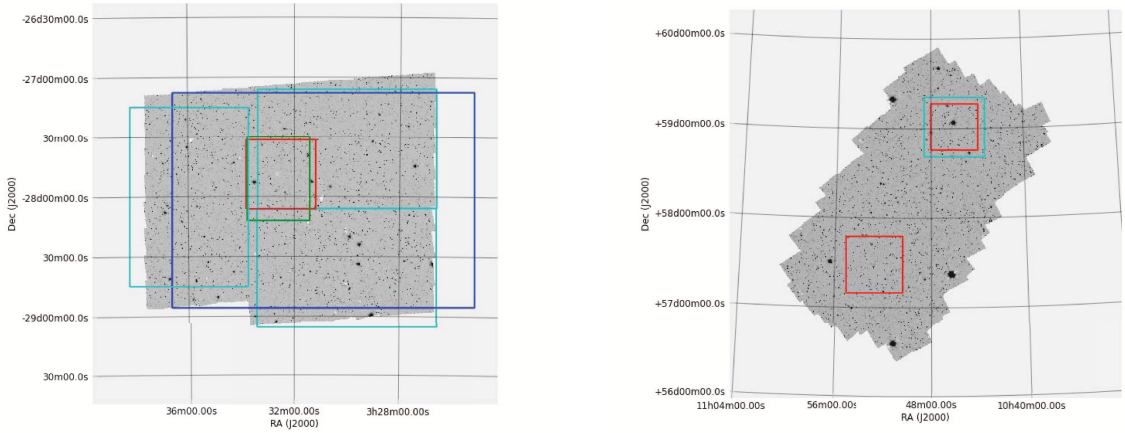

Fig. 3.— *Left* The [3.6] image of the CDFS field. The three VIDEO pointings are in cyan, the SIMPLE/ECDFS field in green, the ATLAS radio survey in blue, and the HerMES level 2 field in red (rotation to be decided). *Right* The [3.6] image of the Lockman field. Superposed are the Owen/Wilkes deep VLA/Chandra field in cyan, the two HerMES level 3 fields in red (rotation to be determined).

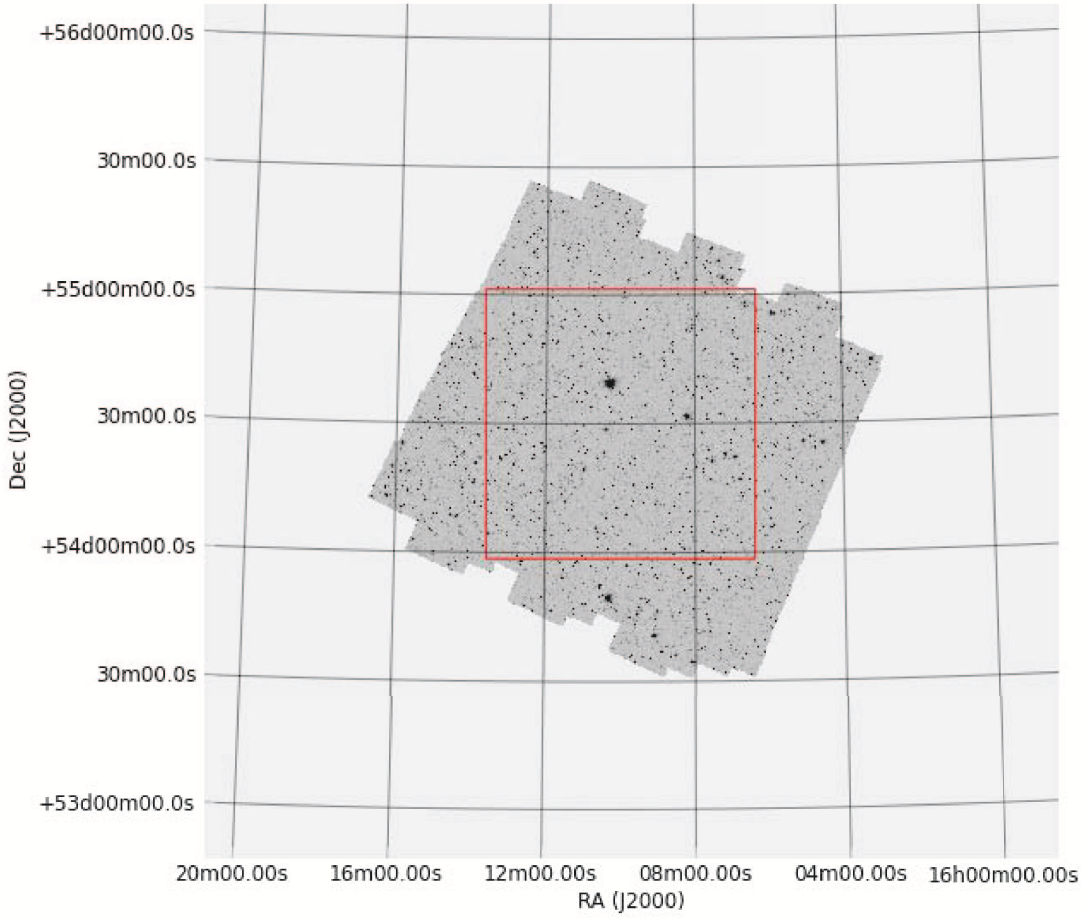

Fig. 4.— The [3.6] image of the ELAIS-N1 field. The HerMES level 5 field is in red (rotation to be determined).

the two epochs ranges from a few days to several months. This allows us to reject asteroids, and also gives us better photometric accuracy by ensuring that most objects will appear in very different places on the array in the two observations. This arises from both a half array offset in array coordinated between the two epochs, and the fact that a few day difference in the execution of each epoch results in a few degree difference in the field rotation. This rotation difference results in a different map grid for the two different epochs (Fig. 1).

2.3.1. Design of the Astronomical Observing Requests (AORs)

Towards the end of the IRAC Warm Instrument Characterization (IWIC), several tests were performed on variations of the SERVS AORs to attempt to establish which observation strategy was optimal. We tested three strategies, all using the small cycling dither pattern, which allows for good coverage whilst ensuring that objects are shifted by a minimum of several arcseconds between observations. The three strategies tried were: (1) two epochs of three dithered 200s frames, (2) two epochs of three dithered pairs of repeated 100s frames, and (3) two epochs of six 100s frames. Strategy (1) is the most efficient, and also, in principle, results in a lower read noise contribution, but in practice artifacts from bright stars were strong, reducing the effective area, and the radiation hit (radhit) numbers were high, resulting in a few radhits leaking through into the final mosaic. There was also no measurable improvement in the noise compared to the other two options, which used 100s frames. Option (2) was only a little less efficient than option (1), but image persistence effects were significant. Option (3) was therefore adopted, resulting in a very robust survey at the expense of only $\approx 3\%$ of extra observing time.

The mapping strategy uses the small cycling dither pattern, which ensures full coverage with our map spacing of $280''$. Each epoch of a SERVS field takes sufficently long to observe that the field rotation changes significantly between the start and end of a single epoch of observations, thus we also needed to be robust against a 7 degree field rotation between AORs (expected in an $\approx$ 10 day window in most SERVS fields). To allow for this, and to allow for accurate filling out of fixed field geometries in all but the ELAIS N1 field, the SERVS AORs were kept relatively small (3×3 maps), and spaced close enough to ensure overlap for the largest expected field rotation. The small AORs also had the advantage of being easier to schedule, allowing the placement of downlinks and the insertion of short non-SERVS observations.

The mean integration time per pixel of the resulting SERVS mosaics is close to the design depth, $\approx$ 1200s. There are, however, both regions of significantly deeper data, where AORs and map dithers overlap, and shallower areas, particularly around the edges, or where

one epoch is affected by scattered light from a field star. Figure 6 shows the histogram of cumulative depth for a typical SERVS mosaic.

2.3.2. Overlap with deeper Spitzer *surveys*

A small fraction of the SERVS area is covered by other deep surveys with IRAC. The areas covered by the SIMPLE survey (PID 20708; PI P. van Dokkum) and the SpUDS survey (PID 40021; PI J.S. Dunlop) have been avoided as far as possible, data from these surveys will be combined with the SERVS data in the final mosaics. A selection of the IRAC [3.6] and [4.5] data from these surveys (both of which also use the 100s frametime) will be added into the final SERVS mosaics to attain an approximately uniform overall depth. There are also two small deep fields which we have tiled over with SERVS, and which we will use for verification purposes. These are AORID 4402688 in Lockman (PID 64; P.I. Fazio), and the overlapping pointings of AORIDs 6005016 (PID 196, P.I. Dickinson) and AORID 10092288 (PID 3407, P.I. Yan) in ELAIS-N1.

2.4. Overlaps with surveys at other wavelengths

Overlaps with existing and surveys in progress are listed in Table 3. Here we provide a more detailed description of some of the most significant (in terms of their overlaps with SERVS) of these surveys.

2.4.1. Optical surveys

A number of optical surveys overlap one or more of the SERVS fields. Among the most significant are the ESO/*Spitzer* Imaging Survey (ESIS) in ELAIS-S1 (Berta et al. 2006; 2008) which reaches depths of 25,25,24.5,23.2 (Vega) in B, V, R, I, respectively, the Canada France Hawaii Telescope Legacy Survey (CFHTLS; both deep and wide pointings in u^*, g, r, i, z in the XMM-LSS field reaching depths of 28.7, 28.9, 28.5, 28.4, 27.0 and 26.4, 26.6, 25.9, 25.5, 24.8 AB magnitudes, respectively), and ancillary SWIRE data in Lockman, ELAIS-N1 and CDFS in a variety of depths and filters, but typically reaching at least $r = 24.5$ (Gonzalez-Solares et al. 2010; Surace et al. 2010).

The *Spitzer* Adaptation of the Red Sequence Cluster Survey (SpARCS) (Wilson et al. 2009; Muzzin et al. 2009) has imaged the entire SWIRE area (excluding the XMM-LSS field which is covered by the CFHTLS) in the $z^{'}$ filter using Megacam on the Canada

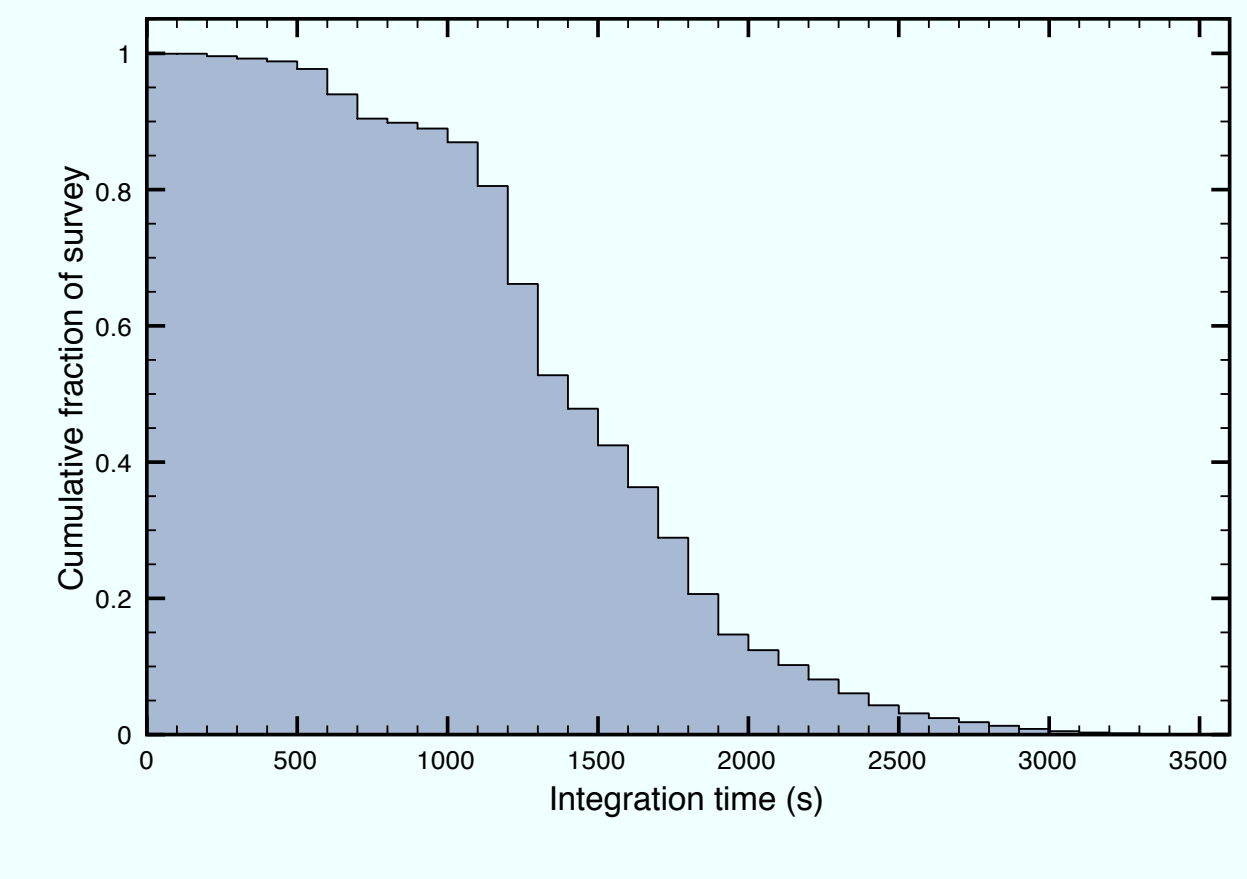

Fig. 5.— The cumulative histogram of integration time per pixel for the ELAIS-N1 field in the [4.5] band. The histogram height for a given integration time represents the fraction of pixels with that integration time or greater.

Table 1: observing log and IRAC Instrument settings for the SERVS fields

Field and epoch	Dates observed	IRAC Campaign(s)	*Spitzer* Program ID	Array Temperatures (K)	[3.6] bias (mV)	[4.5] bias (mV)
ELAIS-N1 epoch 1	2009-07-28 to 2009-08-01	PC1	61050	31	450	450
ELAIS-N1 epoch 2	2009-08-02 to 2009-08-05	PC1	61050	31	450	450
ELAIS-S1 epoch 1	2009-08-06 to 2009-08-11	PC1	61051	31	450	450
ELAIS-S1 epoch 2	2009-08-14 to 2009-08-18	PC2	61051	$\approx 29^*$	450	450
Lockman epoch 1	2009-12-10 to 2009-12-21	PC10,PC11	61053	28.7	500	500
Lockman epoch 2	2009-12-25 to 2010-01-04	PC11,PC12	61053	28.7	500	500
CDFS epoch 1	To be scheduled	-	61052	-	-	-
CDFS epoch 2†	2009-10-16 to 2009-10-28	PC6,PC7	61052	28.7	500	500
XMM-LSS epoch 1	To be scheduled	-	60024	-	-	-
XMM-LSS epoch 2	To be scheduled	-	60024	-	-	-

Notes: * the array temperatures were allowed to float in campaign PC2.

† Epoch 2 of CDFS was observed before epoch 1, which proved to be unschedulable in its originally planned slot.

France Hawaii Telescope (CHFT) or the Mosaic camera on the Blanco Telescope at Cerro Tololo Interamerican Observatory (CTIO). The Megacam observations reach a mean depth of 24.2 AB magnitudes, and the Mosaic camera observations reach a mean depth of 24.0 AB magnitudes (≈ 23.5 in the Vega system).

Optical spectroscopy has thus far been confined to small regions of SERVS, or specific types of objects. The largest spectroscopic survey is the VVDS, which has ≈ 10000 spectroscopic redshifts for field galaxies with $17.5 < I_{\rm AB} < 24$ in their XMM-LSS and CDFS subfields (Le Fevre et al. 2005). In addition, spectra of AGN and quasars, now totaling several hundred objects selected by various techniques, have been obtained in the SERVS fields by Lacy et al. (2007), Ridgway et al. (2010) and Trichas et al. (2010).

2.4.2. Ground-based near-infrared surveys

One of several major surveys to be carried out by the Visible and Infrared Survey Telescope for Astronomy (VISTA) is the five filter near-infrared VISTA Deep Extragalactic Observations (VIDEO) survey (Jarvis et al. 2010), which will cover 12 deg^2 to AB magnitudes of 25.7,24.6,24.5,24.0,23.5 in Z, Y, J, H and K_s filters. The ELAIS S1, XMM-LSS and CDFS SERVS fields are designed to exactly overlap their corresponding VIDEO fields. The combination of VIDEO and SERVS will be a particularly potent tool for the study of galaxy evolution at high redshifts.

The Deep eXtragalactic Survey (DXS) is part of the UKIRT Infrared Deep Sky Survey (Lawrence et al. 2007), and will cover the Lockman and ELAIS N1 fields to 23.1, 22.7 and 22.5 (AB) in J, H and K respectively. As of 2010 April, Data Release 4 (DR4Plus) is available to the entire astronomical community. It covers parts of the EN1, Lockman and XMM-LSS fields. Data Release 7 is available to the community served by the European Southern Observatory, and includes additional data in the EN1 and Lockman fields.

2.4.3. Mid- and far-infrared, and submillimeter surveys

The SERVS fields were designed to be contained within the SWIRE fields. This has mostly been achieved, although constraints from other surveys mean that a small fraction of SERVS lies outside of the SWIRE coverage.

The HerMES Survey is a Herschel Key Project to survey most of the extragalactic *Spitzer* fields, including the SWIRE fields. HerMES has six levels, corresponding to increasing depths, level 6 being the shallowest (5σ limiting flux density ≈ 55mJy at 160μm) and level 1

the deepest 5σ limiting flux density ≈ 1.7mJy at 160μm, ignoring confusion). All of SERVS is covered to Level 6 or deeper, with significant areas as deep as Level 3 (5σ limiting flux density ≈ 7mJy at 160μm). See Oliver et al. (2010) for full details of the HerMES survey.

The wide area component of the SCUBA-2 Cosmology Survey (S2CLS) will cover the XMM-LSS, Lockman, EN1 and CDFS fields. The survey will be performed at 850μm to an root mean square (RMS) noise of 0.7mJy.

2.4.4. Radio surveys

The Australia Telescope Large Area Survey (ATLAS; Norris et al. 2006) overlaps with much of the SERVS fields in ES1 and CDFS. The ATLAS survey, which has not yet finished, will have an RMS of 10μJy and a spatial resolution of ≈ 8 arcsec at 20cm across both fields. A preliminary release of the survey data for CDFS (Norris et al. 2006) and ES1 (Middelberg et al. 2008) has an RMS noise of 30μJy. An image showing the overlap between the SERVS and ATLAS fields can be found in the accompanying paper by Norris et al. (2010).

The EN1 and Lockman fields have been surveyed at 610MHz with the Giant Meter Wave Telescope (GMRT; Garn et al. 2008a,b, respectively). These surveys read a mean RMS of $\approx 60\mu$Jy at a spatial resolution of $\approx 6''$.

The Very Large Array (VLA) has conducted several surveys in the SERVS fields. The Lockman field includes the deepest radio survey at 1.4GHz to date, a single $40' \times 40'$ pointing centered at 161.5d, +59.017d, reaching a $5-\sigma$ detection limit of 15μJy near the center of the primary beam (Owen & Morrison 2008), and further deep coverage by Ibar et al. (2009). Simpson et al. (2006) have surveyed the SXDS region with the VLA to a detection limit of 100μJy, and Bondi et al. (2007) have surveyed the VVDS field in XMM-LSS at both 610MHz with the GMRT and 1.4GHz with the VLA to limits of ≈ 200 and 80μJy, respectively. The Faint Images of the Radio Sky at Twenty cm (FIRST) survey (White et al. 1997) covers the Lockman, EN1 and part of the XMM-LSS survey at 1.4GHz to a sensitivity limit of ≈ 1mJy at a spatial resolution of ≈ 5 arcsec.

Two pathfinder telescopes for the proposed Square Kilometer Array are currently under construction in the southern hemisphere. Both these telescopes will undertake continuum surveys which will cover the southern SERVS fields. The Evolutionary Map of the Universe (EMU) survey with the Australian Square Kilometer Array Pathfinder will cover the whole southern sky to 10μJy RMS sensitivity at 1.4GHz with a $10''$ FWHM synthesised beam, and will also have a deep 30 deg^2 pointing to the confusion limit of $\approx 1\mu$Jy RMS, probably in CDFS. The South African Karoo Array Telescope (MeerKAT) has recently had a call

for proposals for deep continuum surveys, among the contenders is the MeerKAT International Giga-Hertz Tiered Extragalactic Exploration (MIGHTEE) survey, which has a strong SERVS participation. MIGHTEE has several tiers, one of which will include the southern SERVS/VIDEO fields to 1μJy RMS at 1.4GHz with an $\approx 5''$ FWHM beam. In the north, the Low Frequency Array (LOFAR) will target the SERVS/SWIRE fields for deep surveys at frequencies of $\sim$ 100MHz.

2.4.5. X-ray surveys

The XMM-LSS field overlaps with the XMM-LSS survey (Pierre et al. 2007) and the Subaru/XMM-Newton Deep Survey (SXDS) (Ueda et al. 2008). Wilkes et al. (2009) have a deep *Chandra* survey overlapping with the deep VLA pointing of Owen & Morrison (2008) in Lockman. In EN1, *Chandra* program 690062 (P.I. Nandra) covers $\approx 1\mathrm{deg}^2$ of the central portion of the field.

2.5. Further ground-based data to be taken by the SERVS team

We are currently obtaining further multiwavelength ancillary data on the SERVS fields with the overall goal of matching the depth of SERVS in shorter wavebands. These data will be made available as part of the overall SERVS public release. We are concentrating on longer optical and near-IR wavebands as these are generally more useful for photometric redshift estimates. In the optical, we are using the SDSS filter set where possible, as the narrower bands allow higher fidelity photometric redshifts than the Johnson-Cousins system (Figure 6). Our target depth in the optical is an AB magnitude $\approx$ 25 and $\approx$ 23 in the near-infrared (the area covered by VIDEO will be significantly deeper than this). Figure 7 shows a comparison of the SERVS depth with those of the other major optical/near-IR surveys planned or in progress.

Observations with SuprimeCam on the Subaru telescope have been carried out in i and z bands as part of the Gemini-Subaru (PI A. Verma) and Keck-Subaru (P.I. S.A. Stanford) time swaps. The z-band observations are concentrated in the northern fields, as VIDEO will cover the southern fields in Z. y We have also begun an imaging campaign with the CTIO mosaic camera, concentrating on the ES1 and CDFS fields in r and i bands.

An H-band imaging campaign, led by M. Lehnert will obtain H-band data with WIRCAM on the CFHT, to match the UKIDSS DXS J and K imaging in the EN1 field. We have applied for time to extend this program to include the Lockman field.

Table 2: The geometry of the SERVS fields

Field Name	Field Center	Field PA (deg)	Field Area (deg^2)	Vertices (degrees)			
ELAIS S1	003748−4400	0	3	10.3,-44.9	10.3,-42.9	8.5,-42.9	8.5,-44.9
XMM-LSS	022000−0448	0	4.5	(37.0,-5.5)	(37.0,-4.1)	(34.0,-4.1)	(34.0,-5.5)
CDFS	033219−2806	0	4.5	54.3,-27.2	51.7,-27.0	51.7,-28.9	54.3,-28.8
Lockman	104912+5807	328	4.0	164.7,57.4	162.2,59.7	159.8,59.0	162.6,56.6
ELAIS N1	161000+5430	350	2.0	244.0,54.2	243.0,55.3	240.9,54.7	241.6,53.6

Note: vertices for XMM-LSS are in parentheses as SERVS data is yet to be taken on this field

Table 3: Surveys at other wavelengths covering ≳10% of a SERVS field (all-sky surveys excepted).

Field Name	X-ray data	Optical Data	Near-IR Data	Mid-IR Data	Far-IR/ submm Data	Radio Data
ELAIS S1	F08[1]	ESIS[2]	VIDEO[3]	SWIRE[4]	HerMES[5] L6	ATLAS[6]
XMM-LSS	XMM-LSS[7] SXDS[8]	CFHTLS[9] VVDS[10]	VVDS[11] UDS[12] VIDEO[3] DXS[12]	SWIRE[4] SpUDS[13]	HerMES[5] L5 S2CLS[14]	VVDS-VLA[15] S06[28]
CDFS	CDFS[16]	SWIRE/CTIO[17] GaBoDS[18] VVDS[10]	VIDEO[3]	SWIRE[4] SIMPLE[14]	HerMES[5] L2,L5 LABOCA/LESS[19]	ATLAS[6] M08[27]
Lockman	W09[20]	SWIRE/KPNO+INT[21] SDSS[22]	DXS[12]	SWIRE[4]	HerMES[5] L3,L5 S2CLS[14]	OM08[23] G08b[24],G10[30] I09[29]
ELAIS N1	N04[25]	SWIRE/INT[20] SDSS[22]	DXS[12]	SWIRE[4]	HerMES[5] L5 S2CLS[14]	G08b[26] Gr08[31]

Notes: [1] Feruglio et al. (2008); [2] Berta et al. (2006, 2008); [3] Jarvis et al. (2010); [4] Lonsdale et al. (2003), Surace et al. (2010); [5] Oliver et al. (2010); [6] Norris et al. (2006), Middelberg et al. (2008); [7] Pierre et al. 2007; [8] Ueda et al. 2008; [9] www.cfht.hawaii.edu/Science/CFHTLS; [10] Le Fèvre et al. (2005); [11] Iovino et al. (2005); Temporin et al. (2008); [12] Lawrence et al. (2007); [13] ssc.spitzer.caltech.edu/spitzermission/observingprograms/legacy; [14] www.jach.hawaii.edu/JCMT/surveys/Cosmology.html; [15] Bondi et al. (2007); [16] Lehmer et al. (2005); [17] www.astro.caltech.edu/∼bsiana/cdfs_opt/, Surace et al. (2010); [18] Garching-Bochum Deep Survey, Hildebrandt et al. (2006); [19] Survey of the CDFS with the Large Apex Bolometer Camera (LABOCA), Weiss et al. (2009); [20] Wilkes et al. (2009); [21] Gonzales-Solares et al. (2010), Surace et al. (2010); [22] Abazajian et al. (2009); [23] Owen & Morrison (2008); [24] Garn et al. (2008b); [25] Chandra proposal 6900602 (P.I. Nandra); [26] Garn et al. (2008a); [27] Miller et al. (2008); [28] Simpson et al. (2006) [29] Ibar et al. (2009) [30] Garn et al. (2010) [31] Grant et a. (2010)

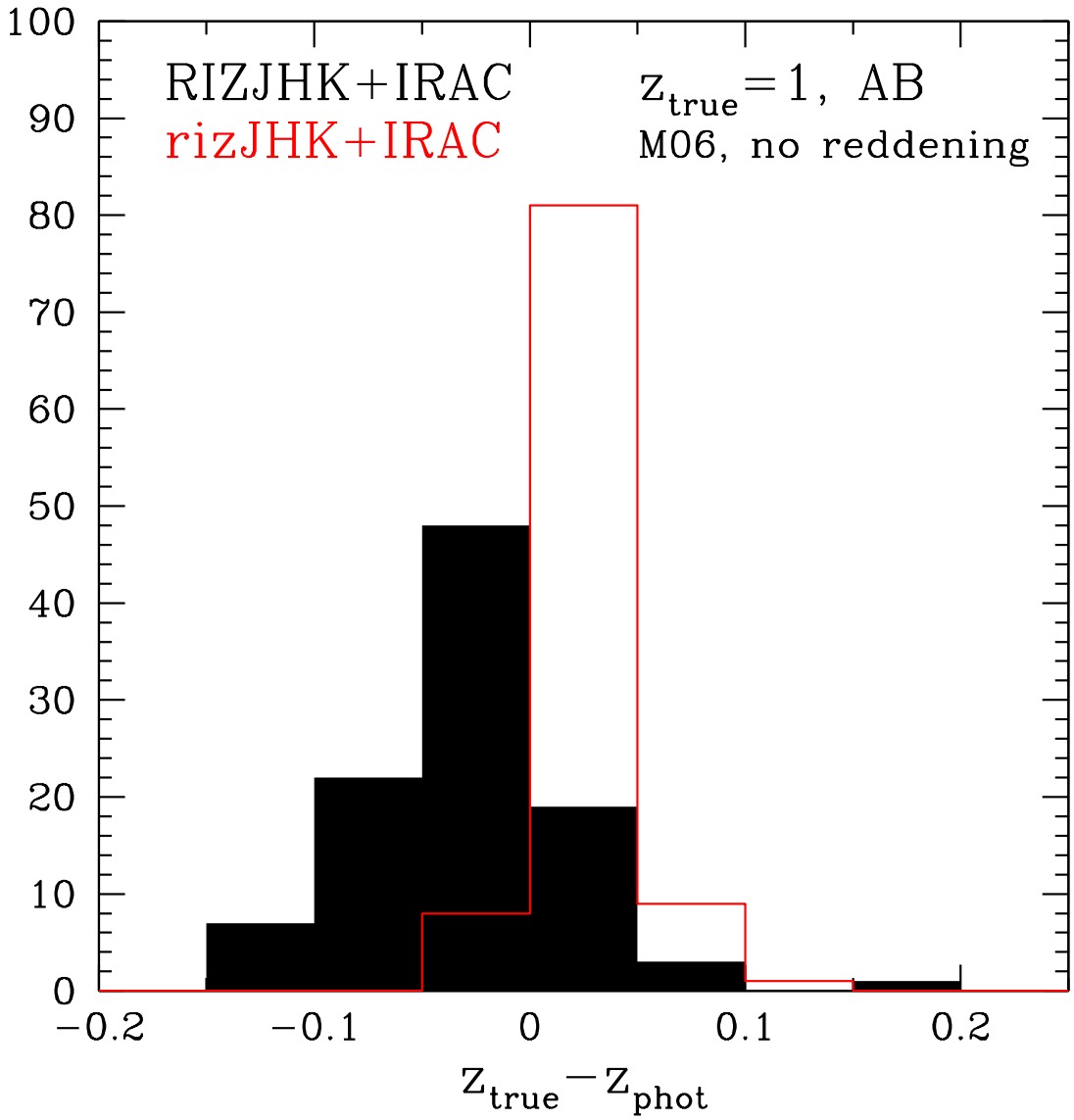

Fig. 6.— Accuracy of photometric redshift as a function of adopted optical filters. A catalog of simulated optical through near-infrared broad band photometry of mock galaxies at a true redshift $z = 1$ from a semi-analytic model (Tonini et al. 2009) was fitted with a wide set of population models from Maraston et al. (2006). The accuracy in recovered photometric redshift is significantly better using the SDSS r, i filters as compared to the from Johnson-Cousins R, I. From Pforr, Maraston & Tonini (2010).

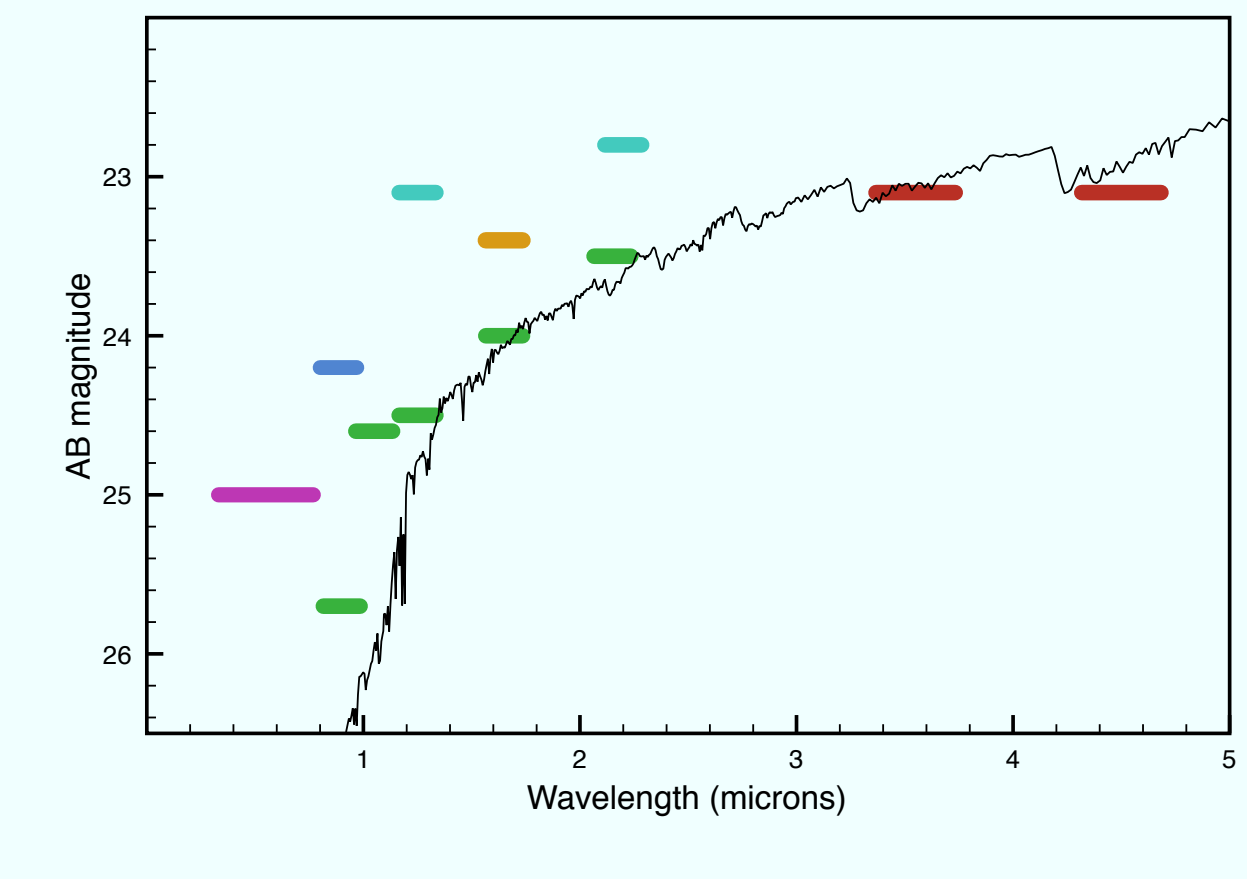

Fig. 7.— Approximate $5-\sigma$ depths of SERVS and near-IR and optical surveys covering the same areas. SERVS is in red, VIDEO green, DXS cyan, CFHT H-band orange, and SpARCS blue. Our target depth for B/g through i-band imaging is shown as the magenta bar (several fields already have imaging to at least this depth). Overplotted is the SED of a 1Gyr old stellar population at $z = 2$ from Maraston (2005).

3. SERVS Observations

Table 1 shows the current status of the survey at the time of writing (April 2010). The first data to be taken, including both epochs of the EN1 field and the first epoch of the ES1 field were taken early in the warm mission, at a lower detector bias than eventually decided on. The effect of raising the detector bias for later observations resulted in a small increase in the detector gain. At [3.6], this gain increase resulted in an $\approx$ 10% increase in sensitivity as the noise on the individual images is dominated by read noise, which is independent of the gain, but at [4.5], which is close to background limited, the gain increase affected the signal and background noise equally, and little or no change in sensitivity was seen. The array temperature was also higher in the early observations, when it was set to 31K, judged to be well above the final equilibrium temperature of the instrument chamber. When it became clear that the equilibrium temperature would be significantly lower than this, the temperature of the detectors was set to 28.7K, which is the temperature which will be used for the remainder of the warm mission. The second epoch of ES1 was taken during the transition from the early warm mission set points to the final ones, and was taken at a floating array temperature of $\approx$ 29K. The effect of the array temperature changes on the sensitivity is small, but it may affect the linearity of the data close to full well.

4. Data analysis

4.1. Images

Data processing begins with the Basic Calibrated Data (BCD) product, produced by the *Spitzer* Science Center (SSC). This consists of images which have been dark subtracted, flat fielded, and have had astrometric and photometric calibration applied. A pipeline based on that used for processing SWIRE was used to further clean the frames of artifacts. Specifically, this pipeline fixed an artifact called "column pulldown" found near bright stars, and also corrected inter-frame bias offsets by setting the background equal to that of a COBE-based model of the zodiacal background (the dominant background at these wavelengths). (Due to the inability to use the IRAC shutter, all IRAC data have offsets from the sky background level which are essentially uncalibratable. Thus no measurement of the true infrared background, nor of any spatial structure within the background larger than the array size of 5 arcminutes, is possible.)

The data were coadded using the MOPEX package available from the SSC. All the data from a single field were coadded onto a single frame; the two different wavelengths are reprojected to the same astrometric projection so that their pixels align one-to-one. The

data are reprojected with a linear interpolation onto a pixel scale of $0.6''$, this provides marginal sampling at 3.6μm. The multiple dithers allow at least some recovery from the severe undersampling of the IRAC camera at these wavelengths.

The initial data provided by the SSC were undercorrected for nonlinearity, and were determined to have small but measurable photometric offsets from the SWIRE data. This is particularly problematic because much of the SERVS data were acquired during the transition from cryogenic to the warm *Spitzer* operations (see Section 3). Since all the SERVS data lies entirely within the area covered by SWIRE, future processing will force the SERVS data directly onto the SWIRE calibration.

5. Simulations

We intend to use semi-analytic models extensively in the SERVS project, both to make testable predictions of the properties of SERVS galaxies, and to inform our follow-up strategies in wavebands other than the near-infrared (e.g. Figure 6). For future SERVS work, we will use two sets of semi-analytic models. That of Henriques & Thomas (2010) and Henriques et al. (2010) use the De Lucia & Blaizot (2007) version of the Munich semianalytic model, which is built on the Millennium dark matter simulation (Springer et al. 2005), but includes a recipe to model tidal stripping of satellite galaxies. This refinement brings it into much better agreement with observations. Stellar population models from Maraston (2005) are used to calculate photometric properties (Henriques et al. 2010). That of van Kampen et al. (2010a) includes both the effects of halo-halo and galaxy-galaxy mergers, and uses GRASIL (Silva et al. 1998) to predict spectral energy distributions from the optical to submm. Mock catalogs from the simulations will be made available as part of the SERVS data release.

6. Primary science goals

6.1. Stellar mass assembly and photometric redshifts

SERVS will ensure the derivation of robust stellar masses because it includes the rest-frame near-infrared out to high redshifts. This coverage is essential to break the degeneracy between star formation history and dust reddening (Maraston et al. 2006). Furthermore, the galaxies detected in SERVS span the epochs where galaxies gain the vast majority of their stellar mass. Brown et al. (2007) and Cool et al. (2008) estimate that L^* galaxies roughly double in mass between $z = 0$ and $z \approx 1$. By comparing galaxy samples at constant number densities, van Dokkum et al. (2010) show that about half the mass of any given large galaxy

is added between $z = 0$ and $z = 2$. SERVS will be able to extend such studies out to higher redshifts with good statistics.

6.2. Obscured star formation

Although SERVS will not be a direct indicator of obscured star formation, overlap with surveys by SCUBA-2 (S2CLS) and *Herschel* (HerMES) will allow more reliable source identification than possible using shorter wavelength data, and better characterization of any extinction of the stellar light, as well as the stellar mass of the galaxy. Based on recent simulations of *Herschel* observations, we expect to detect ~ 700 unconfused sources per deg^2 in ≥ 3 *Herschel* bands (Fernandes-Conde et al. 2008). At the SERVS depths, we expect to detect $> 95\%$ of these sources in both IRAC bands, and thus, with the aid of our ancillary optical and near-infrared data, obtain photometric redshifts and stellar masses for ~ 12000 sources. This will be sufficient to study trends in star formation rate with stellar mass and redshift, for example, to test the idea of "downsizing" of the most actively star-forming galaxies.

6.3. The role of AGN

A unique feature of SERVS is the ability to study rare objects such as AGN and quasars in the context of their environments on Mpc scales. Current models for galaxy formation indicate that AGN and quasar activity play an important role in galaxy formation (e.g. Hopkins et al. 2006), regulating the growth of their host galaxies through feedback. However, the exact nature of this feedback process is unclear. SERVS can help with this problem in several ways. Studies of the galaxy environments in which high redshift AGN and quasars lie can indicate the masses of the dark haloes they inhabit, and also how these masses depend on AGN luminosity and redshift. These can illuminate models for feedback, for example, a preponderance of AGN in massive haloes, accreting at relatively low rates might be an indicator that their host galaxies are no longer growing rapidly (Hopkins et al. 2007). At low redshifts ($z < 0.6$) the SDSS has been used to successfully perform these experiments (Padmanabhan et al. 2009). With SERVS we will be able to take these studies to $z >> 1$.

Nielsen et al. (2010) will investigate the environments of AGN and quasars selected in the mid infrared. We expect to be able to characterize the environments of luminous quasars at $0.8 < z \lesssim 3$ with relative ease, and compare the environments of dust obscured and normal quasars at these redshifts for the first time.

The [3.6] and [4.5] bands are important diagnostics of AGN SEDs, as they are where host galaxy light and hot dust emission from the torus overlap in the SEDs of many dust obscured AGN and quasars at moderate redshifts ($z \sim 1$). In unobscured, or lightly obscured objects, this is where the optical/UV emission from the accretion disk transitions to the hot dust emission. Petric et al. (2010) present SEDs of AGN and quasars selected in the mid-infrared, and use SERVS data to help apportion the different sources of near-infrared light. The luminosities of the hosts themselves, if free from contamination by AGN-related light, can also be used to study the stellar masses of the host galaxies. Huynh et al. (2010) describe the discovery of a population of radio sources with host galaxy fluxes well below the limit of the SWIRE survey, but which are detected or have good limits in deeper IRAC data. They conclude that these are most likely radio-loud AGN with faint host galaxies, but the sample to date is small. Norris et al. (2010) present an initial study of this hitherto unsuspected population with SERVS, including stacking of objects that are too faint to be detected, even in SERVS, and which may represent a very high redshift population.

6.4. The role of environment

SERVS will be a very powerful tool for studying the influence of environment on galaxy formation and evolution. The SERVS areas are already covered by the SpARCS survey, which is successfully finding clusters at $z > 1$ using the red sequence technique applied to SWIRE [3.6] and [4.5] data. We will be able to go deeper into the luminosity function of the SpARCS clusters which are in the SERVS area. In addition, Geach et al. (2010) are pursuing a cluster selection technique using photometric redshifts combined with Voronoi tesselation in an attempt to identify further, mostly lower mass, cluster candidates.

Galaxy-galaxy correlations will also be a valuable probe of galaxy formation. With SERVS we will be able to calculate the galaxy-galaxy correlation over a wide range of luminosities and redshifts. By using the five large, well separated SERVS fields we should be able to average out the effects of large-scale structure on our measurements. van Kampen et al. (2010b) present an initial analysis, showing the evolution of the correlation function between high redshifts ($z > 1.3$) and intermediate redshifts (~ 0.8) using simple [3.6]-[4.5] color cuts.

6.5. High redshift quasars

Although not designed as a survey for $z > 6$ quasars, SERVS will be valuable for constraining the faint end of the quasar luminosity function at high redshifts. The unique multi-band SERVS dataset, in combination with DXS and VIDEO, will allow the rejection of many contaminants of high-z quasar searches on the basis of near-infrared photometry alone. Quasar searches have been or will be carried out in the ELAIS-N1 and Lockman fields where overlap with DXS DR4plus exists, using SERVS, DXS and SpARCS data.

7. Legacy value

Notwithstanding the wide range of science we can already undertake with SERVS, the legacy value of the survey is expected to be immense. No other thermal infrared telescope is planned which will be able to survey as deep and wide as *Spitzer*, and SERVS has a unique combination of area and depth which will ensure its value long into the future. We expect objects selected from SERVS to be picked as targets for telescopes such as *JWST* and ALMA long into the future.

8. Data disemmination

Basic calibrated images from SERVS are available immediately from the *Spitzer* archive. SERVS mosaics and catalogs, including ancillary data at other wavelengths taken as part of SERVS will be made available to the community during the summer of 2012, ultimately through the *Infrared Science Archive* (IRSA). In the meantime, interested parties are welcome to contact the PI to discuss possible collaborations.

9. Acknowledgements

This work is based on observations made with the *Spitzer Space Telescope*, which is operated by the Jet Propulsion Laboratory, California Institute of Technology, under a contract with NASA. Support for this work was provided by NASA through an award issued by JPL/Caltech. JA, HM, MG and LB gratefully acknowledge support from the Science and Technology Foundation (FCT, Portugal) through the research grant PTDC/FIS/100170/2008 and the Fellowships SFRH/BD/31338/2006 (HM) and SFRH/BPD/62966/2009 (LB).

REFERENCES

Abazajian, K.N. et al. 2009, ApJS, 182, 543

Ashby, M.L.N. et al. 2009, ApJ, 701, 428

Berta, S. et al. 2006, A&A, 451, 881

Berta, S. et al. 2008, A&A, 488, 533

Bondi, M. et al. 2007, A&A, 463, 519

Brown, M.J.I., Dey, A., Januzzi, B.T., Brand, K., Benson, A.J., Brodwin, M., Croton, D.J. & Eisenhardt, P.R. 2007, ApJ, 654, 858

Cool, R.J. et al. 2008, ApJ, 682, 919

De Lucia, G. & Blaizot, J. 2007, MNRAS, 375, 2

Fazio, G.G. et al. 2004, ApJS, 154, 10

Feruglio, C. et al. 2008, A&A, 488, 417

Garn, T., Green, D.A., Riley, J.M. & Alexander, P. 2008a, MNRAS, 383, 76

Garn, T., Green, D.A., Riley, J.M. & Alexander, P. 2008b, MNRAS, 387, 1037 Lockman ext

Garn, T., Green, D.A., Riley, J.M. & Alexander, P. 2010, Bull. Astr. Soc. India, in press (arXiv1008:2777

Gonzalez-Solares, E. et al. 2010, in preparation

Grant, J.K., Taylor, A.R., Stil, J.M., Landecker, T.L., Kothes, R., Ransom, R.R. & Scott, D. 2010, ApJ, 714, 1689

Henriques, B.M.B. & Thomas, P.A. 2010, MNRAS, arXiv:0909:2150

Henriques, B.M.B., Maraston, C., Monaco, P., Fontanot, F., Menci, N., De Lucia, G. & Tonini, C. 2010, MNRAS, submitted, arXiv:1009.1392

Hildebrandt, H. et al. 2006, A&A, 452, 1121

Hopkins, P.F., Hernquist, L., Cox, T.J., Di Mattei, T., Robertson, B. & Springer, V. 2006, ApJS, 163, 1

Hopkins, P.F., Lidz, A., Hernquist, L., Coil, A.L., Myers, A.D., Cox, T.J. & Spergel, D. 2007, ApJ, 662, 110

Huynh, M., Norris, R.P., Siana, B. & Middelberg, E. 2010, ApJ, 710, 698

Ibar, E., Ivison, R.J., Biggs, A.D., Lal, D.V., Best, P.N. & Green, D.A. 2009, MNRAS, 397, 281

Ilbert, O. et al. 2006, A&A, 453, 809

Jarvis, M.J. et al. 2010, in preparation

Iovino, A. et al. 2005, 442, 423

Lacy, M. et al. 2007, AJ, 133, 186

Lawrence, A. et al. 2007, MNRAS, 379, 1599

Le Fèvre, O. et al. 2005, A&A, 439, 845

Lehmer, B.D. et al. 2005, ApJS, 161, 21

Mainzer, A.K., Eisenhardt, P., Wright, E.L., Liu, F.-C., Irace, W., Heinrichsen, I., Cutri, R. & Duval, V. 2005, Proc. SPIE, 5899, 262

Maraston, C., Daddi, E., Renzini, A., Cimatti, A., Dickinson, M., Papovich, C., Pasquali, A. & Pirzkal, N. 2006, ApJ, 652, 85

Middelberg, E. et al. 2008, AJ, 135, 1276

Miller, N.A., Fomalont, E.B., Kellerman, K.I., Mainieri, V., Norman, C., Padovani, P., Rosati, P. & Tozzi, P. 2008, ApJS, 179, 114

Muzzin, A. et al. 2009, ApJ, 698, 1943

Norris, R. et al. 2006, AJ, 132, 2409

Norris, R.P. et al. 2010, ApJ, submitted

Oliver, S. et al. 2010, in preparation

Owen, F.N. & Morrison, G.E. 2008, ApJ, 136, 1889

Padmanabhan, N., White, M., Norberg, P. & Porciano, C. 2009, MNRAS, 397, 1862

Petric, A.O. et al. 2010, in preparation

Pforr, J., Maraston, C. & Tonini, C., in preparation

Pierre, M. et al. 2007, MNRAS, 382, 1365

Ridgway, S.E. et al. 2010, in preparation

Sanders, D.B. et al. 2007, ApJS, 172, 86

Silva, L., Granato, G.L., Bressan, A. & Danese, L. 1998, ApJ, 509, 103

Simpson, C.J. et al. 2006, MNRAS, 327, 721

Springel, V. et al. 2005, Nat, 435, 629

Surace, J.A. et al. 2010, in preparation

Temporin, S. et al. 2008, A&A, 482, 81

Tonini, C., Maraston, C., Devrient, J., Thomas, D. & Silk, J. 2009, MNRAS, 396, 36

Trichas, M. et al. 2010, MNRAS, submitted

Ueda, Y. et al. 2008, ApJS, 179, 124

van Kampen, E. et al. 2010a, in preparation

van Kampen, E. et al. 2010b, in preparation

Weiss, A. 2009, ApJ, 707, 1201

White, R.L., Becker, R.H., Helfand, D.J. & Gregg, M.D. 1997, ApJ, 475, 479

Wilkes, B.J. et al. 2009, ApJS, 185, 433

Wilson, G. et al. 2009, ApJ, 698, 1943